CONCEPTUAL DESIGN OF A MOBILE RADIATION SCANNER FOR NUCLEAR SECURITY APPLICATIONS IN MAJOR PUBLIC EVENTS

Débora M. Trombetta[1], Alf Göök[1], Jana Petrovic[1], and Bo Cederwall[1]
[1]*Department of Physics, KTH Royal Institute of Technology, SE-10691 Stockholm, Sweden*

ABSTRACT
There is an increasing awareness of the need for development of effective nuclear security systems in the context of security related to major public events. Such systems include detection of radiation levels that may originate from intentionally placed nuclear - or other radioactive - material by criminal or unauthorised actors.
According to the IAEA-NSS 18 - Nuclear Security Systems and Measures for Major Public Events /Implementing Guide - procedures for background radiation mapping and screening of venues for the detection of nuclear or other radioactive materials outside of regulatory control (MORC) before the major public event are required measures.
We present preliminary results of a conceptual design study for an organic-scintillator-based mobile radiation screening system with improved features that, additionally, enables a signature detection of special nuclear materials (SNM).
Organic scintillators have a high sensitivity to fast neutrons and gamma-rays. Such radiation detector materials with the additional ability to discriminate between the two particle types by means of pulse shape discrimination (PSD) are commercially available in the form of solid plastic scintillators, single-crystal organic scintillators like Stilbene, or liquid scintillators. Detection systems based on such materials are excellent for general-purpose radiation detection with limited radionuclide identification capabilities. In addition, they enable detection of fast gamma-neutron and neutron-neutron coincidences, which is an effective way to determine a clean signature of SNM, since these particles are correlated in time when emitted during the fission process.
The modelling of a mobile scanning system in different conditions is carried out using the Monte Carlo code MCNP6.2.

1. INTRODUCTION

The threat involving the nuclear sector generally consists of the potential for terrorists or violent non-state actors (VNSA) to acquire nuclear weapons-usable material (or a nuclear weapon), as well as the capacity to compromise the safety of a facility housing nuclear materials. In the black market, nuclear and radioactive materials are announced for sale by illegal actors and sought by members of extremist groups [1]. This contributes to the increasing awareness of the need to develop effective nuclear security systems in the context of security related to major public events. Such systems include detection of radiation levels that may originate from intentionally placed nuclear or other radioactive materials by terrorists or VNSA [2]. According to the IAEA-NSS 18 - Nuclear Security Systems and Measures for Major Public Events /Implementing Guide [3] - procedures for background radiation mapping and screening of venues for the detection of nuclear or other radioactive materials outside of regulatory control (MORC) before the major public event are required measures. To perform surveys of large areas portable radiation scanners (PRSs) or backpacks are commonly used, but large detectors mounted inside cars or helicopters can also be applied to survey or search in places like roadways and parking garages [3]. Recently, Unmanned Aerial Vehicles (UAV) are being developed to operate as radiological monitoring in emergency situations [4]. We present preliminary results of a conceptual design study for an organic-scintillator-based mobile radiation screening system that enables enhanced signature detection of special nuclear materials (SNM).

2. METHODS

2.1 Monte Carlo Code

The MCNP6 code, version 6.2 [5], was used to model and simulate the particles' emission and interaction with the medium, in order to investigate the design and the applicability of the proposed technique. The fission model FREYA [6] was used to perform the spontaneous fission modelling. The nuclear fission physics available in the code includes: multiplicity distribution of gamma rays and neutron for each fission, multiplicity dependent energy spectra and angular emission from fission fragments, allowing neutron-neutron, gamma-gamma and gamma-neutron time coincidence calculations [7].

Organic scintillation detectors are capable of detecting neutrons and photons. Some materials have the additional abillity to discriminate between the neutron- and photon-induced signals by means of pulse shape discrimination (PSD). To evaluate detection of individual particles and their correlations in time in the computational environment, the card PTRAC [8] was used. It was considered that every neutron that undergoes elastic scattering and every photon that undergoes Compton scattering, pair production or photo-electric absorption inside the active volume of the scintillator causes a detection. The detection events are subject to thresholds on the deposited energy of $E_{neutron} > 0.5MeV$ and $E_{\gamma} > 0.02MeV$ for neutrons and gamma-rays respectively. A coincidence time window of 100ns was considered for fast time correlations between detected particles.

2.2 System Conceptual Design

The investigated radiation scanner uses four highly efficient EJ-309 liquid scintillation detectors [9] of 12.7 cm x 12.7 cm cylindrical active volume. A schematic view of the detector assembly is seen in Fig. 1. The detectors were separated by 15.2cm center to center, while the distance between the front face of each detector to the ground was consistently 10 cm in this conceptual study.

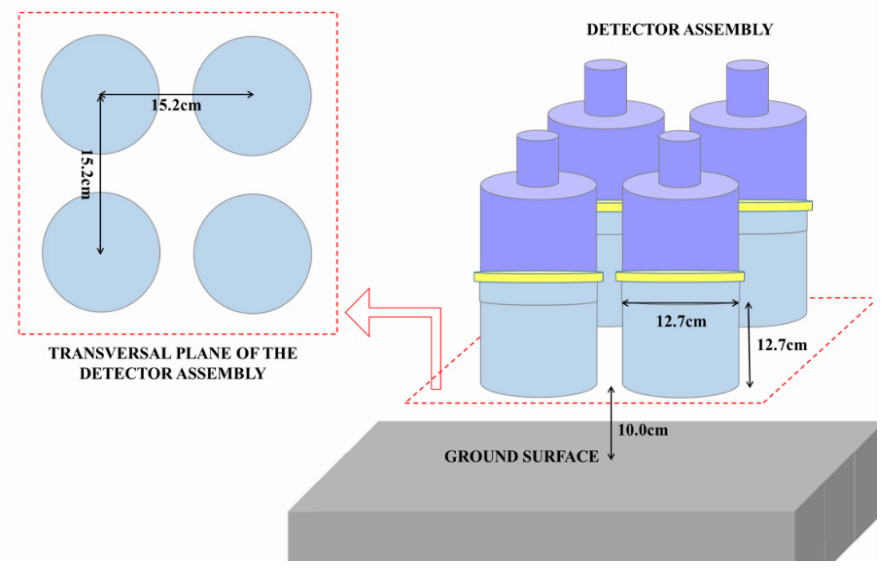

Figure 1: Schematic detector configuration as modeled with MCNP.

2.3 Source Modeling

The nuclear-material source was Pu in four different isotopic compositions. The Pu isotopic weight percentages were taken from the PNNL compendium[10] and are presented in Table 1 along with the total Spontaneous Fission Activity (A_{SF}) for each material .

The source, 100g of metallic plutonium (density 19.84g/cm^3), was modeled as a cylinder with 1cm radius and 1.6 cm height. As mentioned above the emission was modelled using the FREYA fission model and the number of simulated histories were 10^6. Results were normalized to the spontaneous fission source rate.

Table 1: Nuclide weight fractions and total spontaneous fission activity (A_{SF}) for the Pu-source materials investigated.

Source category	**1**	**2**	**3**	**4**
	4-7% Pu-240	10-13% Pu-240	16-19% Pu-240	21-23% Pu-240
Nuclides	**Weight fraction**			
Pu-238	0.0001	0.0009	0.0023	0.0099
Pu-239	0.9363	0.8619	0.7845	0.6237
Pu-240	0.0599	0.1171	0.1651	0.2178
Pu-241	0.0019	0.0099	0.0140	0.1188
Pu-242	0.0003	0.0017	0.0067	0.0297
	A_{SF} (fissions/s)			
	3.03e+03	5.92e+03	8.88e+03	1.40e+04

2.4 Shielding materials

The field condition effects on the detection sensitivity were investigated. As an initial study, soil (earth) was investigated as a potential shielding for the nuclear material. Material of type 105 from the PNNL-15870 [10] compendium was used to represent a dry soil rich in minerals, with 1.52g/cm3 density, 51% of oxygen and around 49% of minerals, such as Na, Mag, Si, K and Ca. Material of type 104 from the same reference was used to represent soil containing 22% of water moisture, with 63% of SiO2, and 15% of Al2O3 (1.52g/cm3 density).

2.5 Background and false coincidences

The use of coincidences is an advantage for measurements in a non-controlled environment with significant background levels of single neutrons and gamma-rays. Literature studies relate time-correlated neutrons and gammas coming from spallation and evaporation reactions of air nuclei - where the gammas can also be generated by electromagnetic cascade showers [11]. For

time intervals shorter than 5 microseconds the Feynman variance for background gamma rays is approximately zero, which means no true time correlations. Davis et al. [12] performed an investigation of the background rates using the same type of organic scintillator detectors and observed a significant increase in the neutron singles rate for different altitudes (0 - 1200m) and a corresponding decrease in counting rate as a function of increasing atmospheric pressure. No significant dependence of neutron singles rate was observed with temperature (ranging from 5ºC till 37ºC) or humidity (ranging from 2 to 16g/m^3). The neutron/gamma misidentification probability for this type of detectors working in PSD mode can be considered around one permille [14]. This factor is dependent on the gamma background rate since pile-up is a contributing factor to PSD errors.

The same type of detectors as modeled in the present study operating in coincidence mode have been tested in laboratory conditions [13,18]. The mean background count rates adopted in the present work have been derived from Ref. 18 for the present detector geometry and amount to 0.500 ± 0.001s^{-1}, 0.00064 ± 0.00004s^{-1}, and 0.00045 ± 0.000002s^{-1} for single neutrons, gamma-neutron coincidences, and neutron-neutron coincidences, respectively.

2.6 Minimum Detectable Amount

When performing measurements with a counting system in a non-controlled environment it is of interest to determine the minimum reliable detection limit related to the equipment. The minimum detectable amount (MDA) [15] of fission activity was calculated for the specific setup geometry in the present work.

The net counts (NS) resulting from a measurement are calculated as the total number of counts (NT) minus the counts measured from the background (NBG) during the same time (Eq.1).

$$NS=NT-NBG \quad \textbf{(Eq.1)}$$

A critical limit (L) is chosen to make a decision whether the detected activity is related to a source or not. It is determined as a compromise to minimize the likelihood for false positive and false negative detections. Therefore, L should be chosen low enough to minimize the possibility of incorrectly discarding real activity detection (false negative, FN), yet high enough not to trigger a false detection when no real activity is present (false positive, FP). In order to have a probability that a sample following a gaussian distribution will assume a value inside the interval of 90%, ensuring that a false positive probability will be lower than 5%, the critical limit was determined by

$$L=1.645\sigma_{NS}=1.645\sqrt{2}\sigma_{BG} \quad \textbf{(Eq.2)}$$

where the considered signal (NS) is small compared to the background (NBG).

To determine the minimum mean value of net counts (ND), two different approaches will be considered. The first one using again the probability lower than 5% - $ND_{5\%}$, and a second one where the probability would be lower than 0.15% - $ND_{0.15\%}$. So ND should be calculated by

$$ND_{5\%}=L+1.645\sigma_{ND(5\%)} \quad \textbf{(Eq.3)}$$

$$ND_{0.15\%}=L+3\sigma_{ND(0.15\%)} \quad \textbf{(Eq.4)}$$

where

$$\sigma_{ND(5\%)}=\sqrt{(2\,NBG\,+\,ND_{5\%})}=\sqrt{2}\,\sigma_{BG}+1.645 \quad \textbf{(Eq.5)}$$

$$\sigma_{ND(0.15\%)}=\sqrt{(2\,NBG\,+\,ND_{0.15\%})}=\sqrt{2}\,\sigma_{BG}+3 \quad \textbf{(Eq.6)}$$

And both ND values are translated to the activity by

$$MDA(ND_{5\%}) = ND_{5\%}/T\,k = (4.653\,\sigma_{BG} + 2.706)/T\,k \quad \textbf{(Eq. 7)}$$

$$MDA(ND_{0.15\%}) = ND_{0.15\%}/T\,k = (3.740\,\sigma_{BG} + 1.288)/T\,k \quad \textbf{(Eq. 8)}$$

where, T is the counting time and k is the probability of detection per fission that is dependent on the system geometry, detectors and surrounding material. In the simulations k is calculated as the ratio between the detected number of particles/coincidences and the number of simulated fission events in the source. The MDA using single neutrons and coincidences between neutrons and gamma-neutron was calculated for different depths and soil conditions.

It is important to highlight that this calculation is based only on counting statistics. We used Poisson counting statistics for estimating the uncertainties in the MDA calculation, which might lead to an overestimation of the detection capabilities in a real measurement. The probability of detection per fission (k) in a real measurement will present associated uncertainties that can be significant compared to Poisson counting errors and are not included here.

2.7 Source localization

Horizontal scanning of an area is useful for determining the lateral position of a detected source. The speed of the moving system also plays an important role for the detection efficiency of the equipment [16]. We here adopt an approach where the system performs each measurement standing still for a defined time and then moves a certain distance to the next position to start a new measurement. However, it is rather straightforward to convert the results to a situation with a continuously moving scanning system. In both cases, the determination of the effective coverage area of the system is essential to define the optimal distance between two consecutive measurements and the scanning speed. Computational simulations of the detector assembly in different lateral positions in the XY-plane relative to the source location were therefore performed to assess the effective lateral coverage and the spatial accuracy that is attainable using lateral scanning. A more accurate determination of the location of SNM in three dimensions (i.e. also the depth/distance away from the detector assembly) can be obtained using the newly developed neutron-gamma tomography approach [17] which is mainly based on the measurement of fast neutron-gamma time correlations. While the method has so far been demonstrated for RPM applications with limited amounts of shielding [17] the spatial resolution with which a source can be localized in the presence of massive shielding, as is potentially the case for the present application, remains to be further studied and will be the subject of future work.

3. RESULTS

The capability of the proposed system in detecting a source buried at different depths was evaluated for two different soil compositions. As can be seen in Fig. 2, the efficiency of the system in detecting gamma-neutron coincidences is around 30 times higher than for neutron-neutron coincidences when the source is at the surface. Both count rates follow approximately exponential curves as a function of depth, with the gamma-neutron count rate showing a steeper slope than the neutron-neutron rate for the dry soil, $0.1405e^{-0.227x}$ and $0.0023e^{-0.245x}$ respectively. This is a consequence of that the gamma-ray transmission is more affected by the minerals in the composition (49%) of the dry soil, i.e. due to the larger presence of material with higher atomic numbers, such as Al, Ti, Mn and Fe.

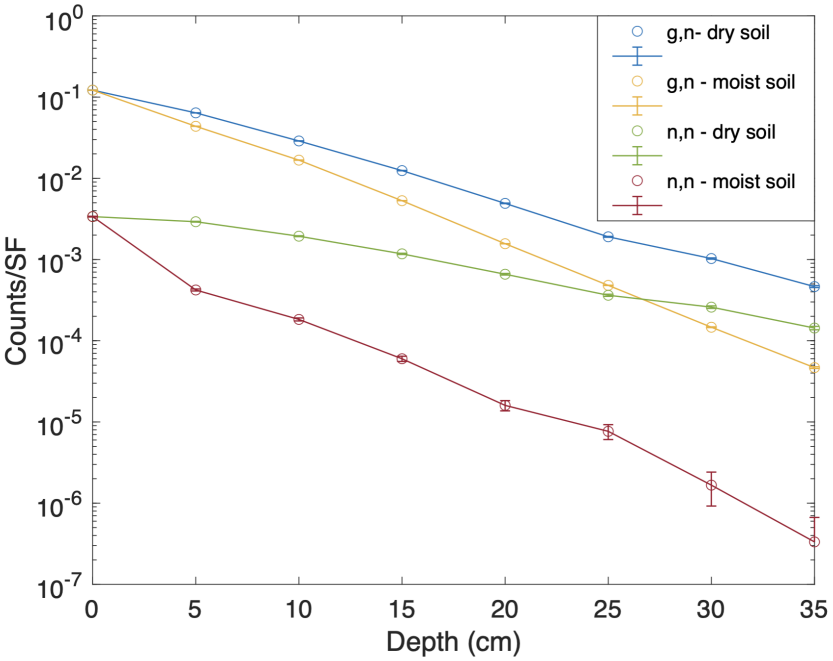

Figure 2: Gamma-neutron and neutron-neutron coincidence detection probability per fission event as function of depth.

However, only at depths larger than about 25 cm does neutron-neutron coincidence counting overtake gamma-neutron counting in efficiency for the presently modeled detector geometry. An inverse effect on the coincidence counting rates as a function of depth is observed for moist soil, where the gamma-neutron coincidence and neutron-neutron coincidence rates follow the respective exponential functions, $0.1339e^{-0.163x}$ and $0.0043e^{-0.095x}$. This effect occurs because gamma-neutron coincidence counting is less affected by the presence of water in the medium. Whereas neutrons are likely to be down-scattered by hydrogen atoms in water, gamma-rays are attenuated by materials with high electron density. Therefore, gamma-neutron coincidences are less affected by the presence of water, compared to neutron-neutron coincidences. Figure 3 shows the shift in the gamma-neutron coincidence time spectra when a source is buried under 25 cm of soil with 22% of water content. The distribution's center of gravity changes from 4.5 ns to 16.5 ns, an increase of more than 10 ns, which is mainly due to the different distance between the source and the detectors, so that both gammas and neutrons need to travel a longer distance to the detectors. A widening in the spectrum also appears since the slower neutrons will take longer time to reach the detectors. An increase in the tail of the distribution is present due to the increased number of interactions between the neutrons and the medium, so called down-scattering.

Fig. 4 presents the normalised single neutron, gamma-neutron and neutron-neutron count rates for source material number 2 (see Table 1) at 5 cm depth in moist soil for different lateral displacements - varying from the central position of the detector assembly until 40 cm distant. The gamma-neutron and neutron-neutron coincidence count exhibit similar behaviour with a relatively steep decrease to around 50% at a distance of 10 cm from position directly below the geometrical center of the detector assembly. The single-neutron count rate shows a somewhat softer decrease as a function of lateral distance, decreasing to 50% at a lateral distance of around 15cm. The narrower lateral response function for coincidence counting will serve to produce sharper lateral positioning during a scan. The main advantage of using fast neutron-gamma coincidence counting, however, is the possibility of 3D localization using the NGET approach [17]. The pitch (or speed) of the

screening should therefore mainly be chosen according to the desirable MDA and the total available measurement time.

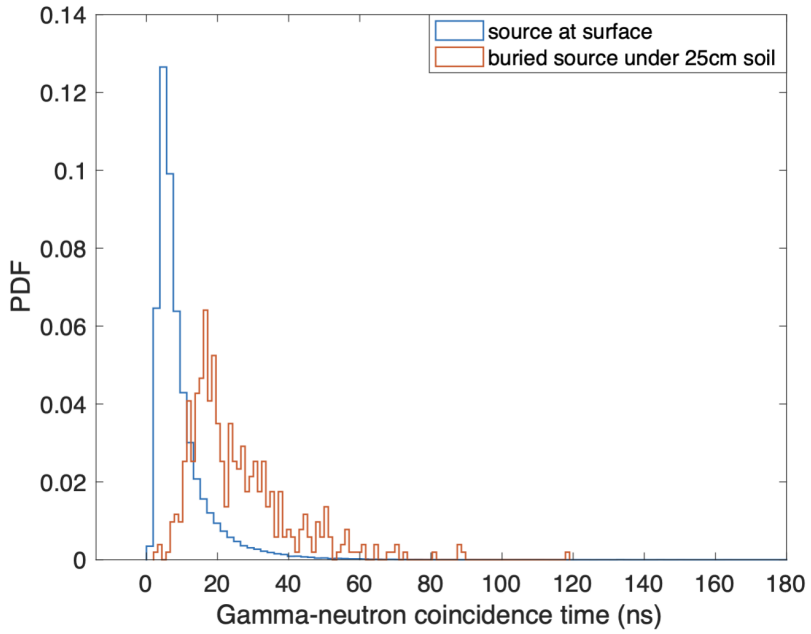

Figure 3: Gamma-neutron coincidence time distributions for a WGPu (10-13% Pu-240) source of 100g in the surface condition and buried under 25cm of soil (22% of water).

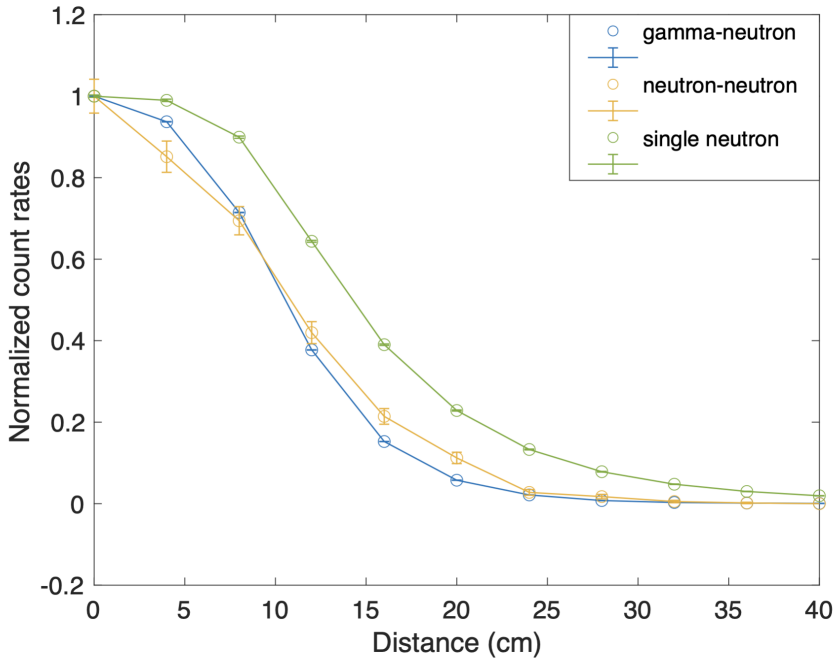

Figure 4: Normalized single-neutron, gamma-neutron and neutron-neutron coincidence count rates for a small pellet as function of the source material's lateral location. The maximum counts calculated for gamma-neutron, neutron-neutron and single neutrons were 294 cps, 3.4cps and 706 cps, respectively .

Table 2 shows derived MDA values for single-neutron detection as well as for gamma-neutron, and neutron-neutron coincidences when the detector assembly is positioned 10 cm above ground and measures during 1 s in each position. For nuclear material at the surface, the calculated MDAs for

gamma-neutron coincidences are similar to single-neutron counting for 5% and 0.15% probability of FN, around 5 fissions/s and 10 fissions/s, respectively. For the nuclear material buried under dry soil, single-neutron counting performs better than coincidence counting. The MDA for single neutron counting is about a factor of three smaller than gamma-neutron counting while it is about a factor of more than 100 smaller than neutron-neutron counting in this case. For moist soil (containing 22% of water in this study) the single- neutron MDAs are similar to those for gamma-neutron coincidences; more than 100 fissions/s are necessary to detect the material buried under 20 cm moist soil through gamma-neutron coincidences or single neutrons for a 1-second measurement time within 5% probability of FP or FN. Neutron-neutron coincidences present the higher MDA for all evaluated cases. For scenarios with elevated neutron background both the single-neutron and gamma-neutron MDAs will increase. It is however expected that the gamma-neutron MDA will increase significantly slower with increasing neutron background due to the fast coincidence requirement.

Table 2: Calculated MDA values for coincidences and single neutrons for 1s measurement time.

	MDA ($ND_{5\%}$) (fissions/s)			**MDA ($ND_{0.15\%}$) (fissions/s)**		
Measurement time =1s	**Source at surface**	**Buried source - under 20cm**		**Source at surface**	**Buried source - under 20cm**	
		dry soil	**moist soil**		**dry soil**	**moist soil**
gamma-neutron	5	45	106	12	115	269
neutron-neutron	711	2.0e+03	4.0e+04	688	2.0e+03	4.0e+04
single neutron	5	15	124	9	30	240

Considering the SF activity calculated for the four sources according to their respective plutonium nuclide percentages (Table 1), a mass range representation related to the MDA($ND_{5\%}$) was calculated and is presented in Table 3. The lower limit corresponds to the isotopic composition of source number 4 and the high limit for the composition of source number 1.

Table 3: Detectable mass ranges related to calculated MDA values for coincidences and single neutrons for 1s measurement time.

	Mass(g)		
Measurement time =1s	**Source at surface**	**Buried source - under 20cm**	
		dry soil	**moist soil**
gamma-neutron	< 1	<1 - 1.5	1 - 4
neutron-neutron	5 - 23	14 - 65	276 - 1,300
single neutron	< 1	< 1	1 - 4

4. CONCLUSIONS

Considering a risk-based approach in a high-risk target event, required nuclear security practices include the screening for nuclear and radioactive materials of venues before lockdown. An essentially unattended scanning procedure using a system as discussed in the present work could aid in the identification of threats with minimum human intervention, higher speed and efficiency. In this paper initial results on the investigation of a conceptual design for a radiation scanner that uses organic scintillators as an alternative to conventional ^{3}He tubes for neutron detection with the objective of identifying the presence of nuclear materials is presented. The proposed design, consisting of four organic liquid scintillator detectors, showed good results for the use of single neutrons and gamma-neutron coincidences. Results based on computational simulations show that it would be able to detect Pu sources with less than 1 gram in 1s measurement time when the source is at the surface. When the source is buried under 20cm of dry and moist (22% water) soil the detectable masses are the order of 1g to 4g of Pu for the same measurement time. Neutron-neutron coincidences were also evaluated, but present considerably lower detection rates.

Future studies are needed for other types of shielding materials such as concrete. Further work to evaluate the performance at elevated background levels should also be performed. Beyond the present security application, other fields of interest include radiological emergency response and environmental surveying, such as localization of lost sources or characterization of sites with large areas of radioactive contamination. An important advantage related to the use of coincidence detection is the low background count rate. The main advantage of including measurements of fast-neutron-gamma time correlations in the operation of the scanning system will, however, be the ability to automatically produce accurate 3D images of SNM using the neutron-gamma emission tomographic technique [17]. The detailed evaluation of imaging performance in the presence of heavy shielding will therefore also be an essential part of future studies.

REFERENCES

1. Truls Hallberg Tonnessen, Islamic State and Technology - A literature Review, Vol 11, No. 6 (2017).
2. Robert Downes, Christopher Hobbs & Daniel Salisbury (2019) Combating nuclear smuggling? Exploring drivers and challenges to detecting nuclear and radiological materials at maritime facilities, The Nonproliferation Review, 26:1-2, 83-104, DOI: 10.1080/10736700.2019.1610256.
3. IAEA nuclear security series, ISSN 1816–9317 ; no. 18.
4. Webpage:https://www.iaea.org/newscenter/news/now-available-new-drone-technology-for-radiological-monitoring-in-emergency-situations, Accessed on April, 11, 2021.
5. MCNP® USER'S MANUAL Code Version 6.2 Los Alamos National Laboratory report LA-UR-17-29981 (October 2017).
6. J.M. Verbeke, J. Randrup, R. Vogt, Fission Reaction Event Yield Algorithm, FREYA — For event-by-event simulation of fission, Computer Physics Communications, Volume 191, 2015, Pages 178-202.
7. M. E. Rising, "CGMF & FREYA Verification in MCNP6" - LA-UR-16-27710, Los Alamos National Laboratory, 2017.
8. L. G. Evans, M. A. Schear, J. S. Hendricks, M. T. Swinhoe, S. J. Tobin, S. Croft, A New MCNP PTRAC Coincidence Capture File Capability: A Tool for Neutron Detector Design, (Los Alamos National Laboratory, Phoenix, AZ, USA, 2011; https://permalink.lanl.gov/object/tr?what=info:lanl-repo/lareport/LA-UR-11-00701).
9. Eljen Technology, Neutron/gamma PSD liquid Scintillator EJ-301, EJ-309, (n.d.) <http://http://www.eljentechnology.com/products/liquid-scintillators/ej-301-ej-309> (accessed 17 November 2017).

10. RJ McConn, Jr CJ Gesh, RT Pagh, RA Rucker, RG Williams III, Compendium of Material Composition Data for Radiation Transport Modeling - PNNL-15870 Rev. 1, 2011).
11. Miloshevsky, G., Hassanein, A., “Time correlation of cosmic-ray-induced neutrons and gamma-rays at sea level”, NIM A, Vol.737. pg.33-41, 2014.
12. Davis, J.R., Brubaker, E., Better, K. Fast neutron background characterisation with the Radiological Multisensor Analysis Platform (RadMap), Nucl. Instrum. Meth. Res. A 858, (2017) 106.
13. Trombetta, D.M., et al., Sensitive detection of special nuclear material based on gamma-fast neutron coincidence counting for RPM application, International Conference on Nuclear Security 2020 proceedings, IAEA)
14. Cederkäll, J., et al. Nucl. Instrum. Meth. Phys Res. A. 385 (1997) 166.
15. Knoll, Glenn F., Radiation detection and measurement - 3rd ed.
16. J.T. Falkner C.M. Marianno, "Validating a Methodology that Associates Minimum Detectable Activity with Detector Velocity", *Journal of Health Physics*, 121,1 (2021)
17. Jana Petrović, Alf Göök, and Bo Cederwall, ’Rapid imaging of special nuclear materials for nuclear nonproliferation and terrorism prevention’, Science Advances, Vol. 7, no. 21, eabg3032 (2021).
18. J. Petrovic et al, these Proceedings.